A Software Tool for Semi-Automated Quantification of Pituitary Volumes

Z. J. Wang[1,2], D-J. Wang[3], J. M. Chia[4], Q. Yuan[1], M. C. Morriss[1,2], and N. K. Rollins[1,2]
[1]University of Texas Southwestern Medical Center, Dallas, Texas, United States, [2]Children's Medical Center, Dallas, Texas, United States, [3]Children's Hospital of Philadelphia, Philadelphia, Pennsylvania, United States, [4]Philips Healthcare, Cleveland, Ohio, United States

Introduction:
The pituitary gland, or hypophysis, is the master gland of the endocrine system. The anterior and posterior pituitary are distinct glands with different embryologic origins and produce different hormones. The volume of the anterior pituitary may decrease as a result of iron overload in thalassemia patients receiving long-term blood transfusion therapy, and this is correlated with hypogonadotropic hypogonadoism(1,2,3). Reliable measurement of the anterior pituitary volume is important for assessing the damage to the pituitary gland in this patient population. Although many software tools are available for brain volumetric analysis, most are for white and gray matter segmentation and not applicable for pituitary volumetry. An automatic approach is non-trivial due to various neighboring regions. The anterior pituitary has interfaces with the posterior pituitary, CSF and the air/bone space of the sphenoid sinus that each requires a different threshold value. Measurement of the anterior and posterior pituitary volumes by manual tracing on MR images can be time consuming and has poor reproducibility. We have developed a semi-automated approach that combines manual tracing and threshold settings based on histograms that simultaneously measures the anterior and posterior pituitary volumes.

Materials and Methods:
MRI data: MRI data free of motion related blurring in the hypothalamus came from an NIH sponsored study of normal brain development (http://www.bic.mni.mcgill.ca/nihpd/info/). Data from 25 subjects were used for testing (12 male, 13 female, age: 5.0~18.3 years, median: 12.5). The data were acquired with 3D RF spoiled FFE (1mm^3 isotropic voxel, TR=22-25 ms, TE = 10-11 ms, flip angle =30^o)(4).
Overall strategy: 2 primary ROIs, one for the anterior and one for the posterior pituitary gland, are first specified to contain the entire gland and its boundary. The gland volume within these ROIs is determined by setting signal threshold values. A target gland may have several different neighboring compartments with different threshold values needed for tissue segmentation. For this reason, additional interfacial ROIs are needed, each containing one type of interface. Tissue segmentation is done at the interface inside these ROIs. Histograms are calculated separately for anterior pituitary, posterior pituitary, CSF space, and air/bone space. The interface threshold setting is the average of the peak positions from the histograms of the two neighboring compartments. There are remaining regions not contained in an interfacial ROI (e.g., at the right or left site of pituitary next to cavernous sinus) where the boundary is determined by manual tracing only.
Software implementation: The software tool was written in IDL. 3D isotropic MR images were interpolated into a spatial resolution of 1/6 mm and displayed in axial, sagittal, and coronal planes simultaneously with a graphical user interface menu. Manual tracing is performed using multiple sagittal and axial planes selected by the operator. The computer routine combines the tracing to obtain a 3D region of interest. This two-plane tracing approach is used because different boundaries are best visualized on different orientations. For example, the boundary of the left and right side of the pituitary gland from the adjacent cavernous sinus is easy on the axial plane but difficult on the sagittal plane. Several ROIs are traced manually: (1) the entire anterior pituitary and its boundary, (2) the entire posterior pituitary and its boundary (the overlapping region between these two ROIs is the interface ROI between the two tissues). (3) the interface between air/bone and anterior pituitary (if present), (4) the interface between air/bone and posterior pituitary (if present). (5) the interface between CSF and anterior pituitary (if present), (6) the interface between CSF and posterior pituitary (if present). (7) an area containing CSF only, (8) an area containing air only. The anterior and posterior ROIs are eroded to contain only pure tissue to generate tissue specific histograms. From these and the histograms of CSF and air space, thresholds between various compartments are calculated. The anterior and posterior pituitary volumes are then obtained. One data set can be processed in 20 minutes or less.

Results:
The anterior and posterior pituitary volumes measured by two operators (V_{1a}, V_{1p} and V_{2a}, V_{2p}) showed excellent agreement (Figure 1).
Anterior pituitary: The average anterior pituitary volume, $(V_{1a}+V_{2a})/2$, ranged from 163 to 719 mm^3, reflecting developmental change over the age range and gender difference. Regression analysis yielded $V_{2a} = 2.2+1.027 \cdot V_{1a}$ (mm^3). The volumes obtained by the two operators were strongly correlated ($r = 0.989$). The average discrepancy between the two operators was 6.2%.
Posterior pituitary: The average posterior pituitary volume, $(V_{1p}+V_{2p})/2$, ranged from 30 to 106 mm^3. Regression analysis yielded $V_{2p} = 8.0+1.008 \cdot V_{1p}$ (mm^3). The volumes obtained by the two operators were strongly correlated ($r = 0.899$). The average discrepancy between the two operators was 16.7%.

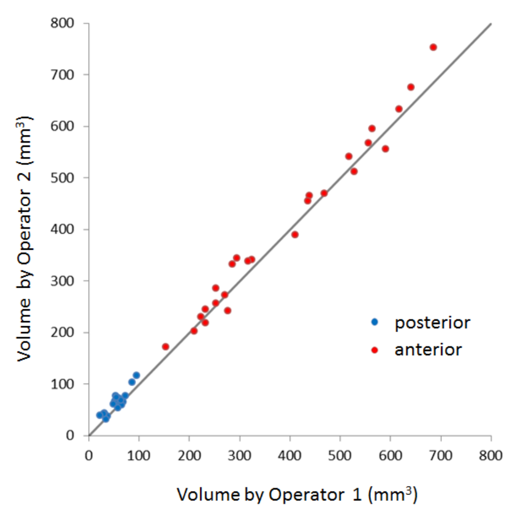

Figure 1. Correlation of the anterior and posterior pituitary volumes measured by 2 operators independently. The solid line is a guide for the eyes with slope = 1.

Discussions and Conclusion:
The software enables reproducible quantification of anterior and posterior pituitary volumes. The method will satisfy the clinical need to evaluate decreases in anterior pituitary volume due to iron overload in thalassemia patients.

References: **1**. Chatterjee R, et al., Ann N Y Acad Sci (1998) 850: 479-82. **2.** Argyropoulou MI, et al., Neuroradiology (2001) 43: 1056-8. **3.** Wang ZJ, et al., Blood (2006) 108(11) 505A. **4.** Evans AC, et al., NeuroImage (2006) 30: 184-202.